# Thermodynamics and Dynamics of Metallic Glass Formers: Their Correlation for the Investigation on Potential Energy Landscape

**Lina Hu,* Xiufang Bian, Weimin Wang, Guangrong Liu, and Yubo Jia**

*Key Laboratory of Liquid Structure and Heredity of Materials, Ministry of Education, Shandong University (south part), Jinan 250061, P.R. China*

*Received: May 16, 2005*

Great progress has been made in basic features of the potential energy landscape (PEL) theoretically. The present work, however, attempts to cast new light on it from experimental aspects. By a survey of experimental data related to thermodynamics or dynamics of metallic glass-forming liquids, it is found that the increased rate of excitation of vibrational entropy at glass transition tends to increase the rate of generation of configurational part. Although for the type of metallic materials a generally positive relationship exists between the density of the energy minima at glass transition and the liquid fragility strength, just as expected, our main attention is paid to the phenomenon of the scattering of the slopes. Analysis shows that the phenomenon results from the different average height of energy barriers between minima near glass transition. Investigation on the PdNiP metallic system indicates that the mismatch entropy is a dominant factor in the barrier height: a large value of it results in low energy barriers. Our previous work on the AlNiCe system gives the support to this finding.

## 1. Introduction

The nature of the transformation by which a supercooled liquid freezes to a glass—the glass transition—is a central issue in condensed matter physics. To gain insight into it, a lot of work[1−3] has been done on the factors that control the viscous properties or the entropy changes as the glass transition is approached, e.g., on the nature of the vitrification. The "Kauzmann paradox"[4] and the success of the "Adams−Gibbs" equation[5] to some degree have both suggested that the nature is not based on one aspect (thermodynamics or dynamics), but it should be the combination of the two aspects that is correlated. Thus, it is of importance to investigate the correlation between the dynamics and the thermodynamics in disordered systems.

Potential energy landscape (PEL) has been thought of as an ideal method to synchronously display the two aspects of properties. In the PEL, the average energy of the minima visited at certain temperature reflects the thermodynamics, and the landscape topology controls the dynamics. Although every substance has its own energy landscape with distinct features, it has been believed that uncovering the topographic nature of the scaling relationship between basin minima and saddle points holds the key to understanding the relationship between dynamics and thermodynamics in deeply supercooled liquids. Equally important is the investigation on how these basic landscape features depend on particle (molecular or atom) architecture or other microproperties that involve details of particle interaction and arise from the nature of real particles.[6]

Numerical investigations of the sampled configuration space in PEL have been performed for several models of liquids.[7−12] An important outcome of these studies is the demonstration that on cooling the system populates basins of the potential energy surface (PES) associated with local minima of deeper and deeper depth.[9] The density of distinct basins with the same depth in bulk systems, as well as the averaged distance between neighboring minimum points in the configuration space, has also been evaluated.[11,13] This information has been incorporated into detailed description of the thermodynamics or the dynamics of supercooled liquids.[8,9,11] Although the achieved progress is exciting, most of the analysis on the PEL is just theoretical. No more information could be obtained concerning how the correlation between thermodynamic and dynamic properties is exhibited by the PEL. To meet the major challenge to the quantification of this descriptive picture, only work on simplified models is not enough. The information from physical experiments equally needs to be taken into account since it helps to uncover the nature of the PEL further.

In the present work, we focus on the particle interaction-induced changes of the basic features of PEL. Selecting metallic materials as the investigated objects is based on the following consideration: the wide usage of bulk metallic glasses as engineering materials urgently requires understanding the nature of the glass transition and how to control the supercooled degree of metal liquids.[14] At the same time, however, available literature on the PEL mostly focuses on small molecules, ionic glasses, or polymers.[13,15,16] Seldom are materials with metallic bonds mentioned. For the type of metallic glasses, dielectric measurements are not possible and the relaxation time usually is measured by shear viscosity and by the determination of the glass transition temperature ($T_g$) using calorimetry at various heating rates.[17,18]

## 2. Experimental Data Evaluation

A search of the literature for thermodynamic and dynamic quantities of metallic glasses has been conducted. For metallic glass formers, the values of the heat capacity changes caused by the glass transition ($\Delta C_{p,s-l}$), the calorimetric glass transition temperature for a scanning rate of 20 K/min ($T_{g,20}$), and the characteristic temperature ($T_0$) are taken directly from the literature[19−34] as shown in Table 1. The characteristic temper-

* To whom correspondence should be addressed. E-mail: hulina0850@mail.sdu.edu.cn. Telephone: 086-531-8392748. Fax: 086-531-8395011.

10.1021/jp052561o CCC: $30.25 
Published on Web 06/28/2005

**TABLE 1: Heat Capacity Change ($\Delta C_{p,s-l}$, cal/mol·K) for 24 Metallic Glass Formers at the Calorimetric Glass Transition Temperature for a Scanning Rate of 20 K/min, $T_{g,20}$[a]**

| metallic glasses | $\Delta C_{p,s-l}$ | $T_{g,20}$ | $T_0$ | $m$ | ref no. |
|---|---|---|---|---|---|
| $Pd_{36.5}Ni_{36.5}P_{27}$ | 3.8 | 635 | 549[b] | 62 | 19, 20 |
| $Pd_{37.5}Ni_{37.5}P_{25}$ | 3.5 | 619 | 508[b] | 51 | 19, 20 |
| $Pd_{64}Ni_{16}P_{20}$ | 3.6 | 582 | 437[b] | 51 | 19, 20 |
| $Pd_{16}Ni_{64}P_{20}$ | 4.0 | 587 | 442[b] | 50 | 19, 20 |
| $Pd_{40}Ni_{40}P_{20}$ | 3.7 | 580 | 367[b] | 41 | 19, 20 |
| | | | 390[c] | | 21 |
| $Pd_{48}Ni_{32}P_{20}$ | 3.5 | 582 | 392[b] | 41 | 22−24 |
| $Pd_{77.5}Cu_6Si_{16.5}$ | 3.5 | 635 | | 52 | 19, 20 |
| $Pd_{40}Ni_{10}Cu_{30}P_{20}$ | 4.1 | 575 | | 52 | 20, 25 |
| $Fe_{30.8}Co_{46.2}P_{14}B_6Al_3$ | 4.0 | 724 | 534[b] | 43 | 19, 20 |
| $Pt_{64}Ni_{16}P_{20}$ | 4.3 | 482 | 336[b] | 50 | 19, 20 |
| $Pt_{60}Ni_{15}P_{25}$ | 4.4 | 482 | 348[b] | 50 | 19, 20 |
| $Pt_{56}Ni_{14}P_{30}$ | 5.4 | 498 | 363[b] | 56 | 19, 20 |
| $Pt_{45}Ni_{30}P_{25}$ | 4.3 | 495 | 320[b] | 42 | 22 |
| | | | 317[b] | | 19, 20 |
| $Mg_{65}Cu_{25}Y_{10}$ | 3.7 | 420 | 260[d] | 41 | 20, 26 |
| $Zr_{41.2}Ti_{13.8}Cu_{12.5}Ni_{10}Be_{22.5}$ | 5.4 | 648 | 412[c] | 39 | 20, 27 |
| | | | 413[d] | | 28 |
| $Zr_{65}Al_{7.5}Cu_{27.5}$ | 3.2 | 650 | | 35 | 20, 29 |
| | | | 382[e] | 36 | 29 |
| $Zr_{65}Cu_{17.5}Al_{7.5}Ni_{10}$ | 3.3 | 633 | | 35 | 20, 30 |
| $Zr_{46.75}Ti_{8.25}Cu_{7.5}Ni_{10}Be_{27.5}$ | 4.4 | 633 | 381[d] | 34 | 20, 31 |
| | | | 372[f] | | 32 |
| $La_{55}Al_{25}Ni_{20}$ | 2.9 | 480 | 262[e] | 32 | 20, 33 |
| $Au_{76.9}Ge_{13.65}Si_{19.45}$ | 5.5 | 295 | 234[c] | 60 | 20, 34 |
| $Au_{77}Ge_{13.6}Si_{9.4}$ | 5.8 | | | 53 | 20, 34 |
| $Ni_{75}P_{16}B_6Al_3$ | 3.5 | 691 | | 53 | 19, 20 |

[a] For $La_{55}Al_{25}Ni_{20}$, $Zr_{65}Cu_{17.5}Al_{7.5}Ni_{10}$, and $Au_{77}Ge_{13.6}Si_{9.4}$, the scanning rates are 40, 10, and 10 K/min, respectively. $T_0$ is the VFT temperature (see eq 1). The fragility parameter, $m$, is calculated at the given $T_{g,20}$. The superscript means the different method by which the viscosity data of the supercooled liquid is obtained. [b] The calorimetry at various heating rates; [c] continuous-strain-ratetensile measurement; [d] Three point beam bending; [e] Dynamic mechanical analyzer; [f] Parallel plate rheometry;

ature $T_0$ is introduced through the VFT equation[35,36]

$$\eta = \eta_0 \exp\left[\frac{B}{T - T_0}\right] \quad (1)$$

where $\eta_0$, $B$, and $T_0$ are fitting parameters and $T$ is the temperature. The measurements of $\Delta C_{p,s-l}$ and $T_{g,20}$ are shown in Figure 1. In Figure 1, $C_{p,l}$ represents the specific heat of the supercooled liquid with an internal equilibrium state and $C_{p,s}$ is that of the quenched sample heated once to the temperature just above $T_g$ at a scanning rate of 20 K/min. The $C_{p,s}$ is unaffected by thermal history and consists of configurational contributions. The $\Delta C_{p,s-l}$ values of most alloys in Table 1 come from the same reference and the similar experimental conditions make them comparable. For the other alloys, the $\Delta C_{p,s-l}$ values are obtained from the figures by eye-determination. In this case, to make $\Delta C_{p,s-l}$ more believable, we try to determine the value of $\Delta C_{p,s-l}$ by referring to several references (such as for ZrCuAl and ZrCuAlNi alloys).[29,30,38] Although the unavoidable error is discouraging, it is less than 2 J/mol·K. Besides, we find that for the same alloy (for example ZrTiCuNiBe in Table 1), the different methods based on using loads on amorphous samples tend to give very similar values of $T_0$. Even though there is a distinct difference in the values of $T_0$ between the calorimetric method and the mechanical method (see $Pd_{40}Ni_{40}P_{20}$ in Table 1), the difference will become tiny when divided by $T_g$. Thus, the following results according to the values in Table 1 are believable, and the unavoidable error due to eye-determination is taken into account in the discussion part.

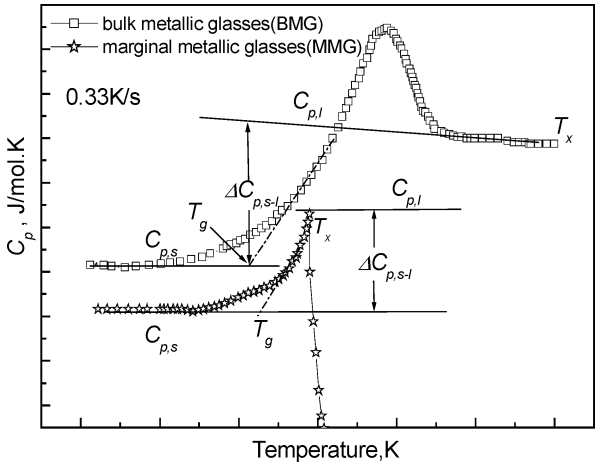


**Figure 1.** Temperature dependence of specific heat of typical metallic glasses. According to the different glass-forming ability, metallic glasses are often divided into two groups: bulk and marginal.[37]

Besides, one widely used dynamic fragility parameter,[39] $m$, has been shown in Table 1 for many systems of metallic glasses. The values of them are mostly derived from Perera's work[20] by using VFT fits to viscosity data in the temperature range close to and below the calorimetric $T_g$. Comparisons in the $m$ of $Zr_{65}Al_{7.5}Cu_{27.5}$ between different reports[20,29] indicate that for metallic alloys the system of the fragility values given by Perera is more reliable than that given by Komatsu[40] which is in the range of 86−121.

## 3. Results and Discussions

**3.1. Correlation of the Basin Shape Changes and the Number of Energy Minima at $T_g$.** Angell[16] has found that thermodynamic fragilities of different liquids are well correlated with their dynamic fragilities. To explain the phenomenon, the idea that the temperature dependence of configurational excess entropy ($S_c$) is the same as that of excess entropy ($S_{ex}$) is often used. The central mind of this idea is that for fragile liquids the influence of the increase in the density of vibrational states undergoing with temperature on $S_c$ is different from that for strong liquids. A much explicit explanation[16] has been plotted as Figure 2, which shows how the change in entropy of a system originates in the change of the energy landscape "basin shape". In Figure 2, for the system with variable basin shape, the generation of extra vibrational entropy ($S_{ex(vib)}$) in the liquid provides an additional drive toward the higher-energy states over that provided by the multiplicity of basins alone. At the same time, the increased rate of excitation of vibrational entropy increases the rate of generation of configurational part, as well as that of the excess entropy. Reports on the possible correlation between liquid fragility and the density of vibrational states[41−43] have suggested that the proportion of $S_{ex(vib)}$ in $S_{ex}$ should reach about 50% for fragile liquids and that for strong liquids the proportion should be very small and even reach zero. However, at present, to separate the configurational part from the vibrational part by experimental or theoretical methods seems impossible. So the idea depicted in Figure 2 is only regarded as a prediction, which requires further support by experiments on real glass-forming liquids.

Then in order to test the prediction, we focus on two values: $\Delta C_{p,s-l}$ and $T_0/T_g$. $\Delta C_p$ is directly related to the configurational entropy, $S_c$, which is determined by the plethora of possible distinct packing states accessible at the temperature $T$.[44] Comparisons of $\Delta C_{p,s-l}$ among different materials can manifest the different changes of the configurational excess entropy due

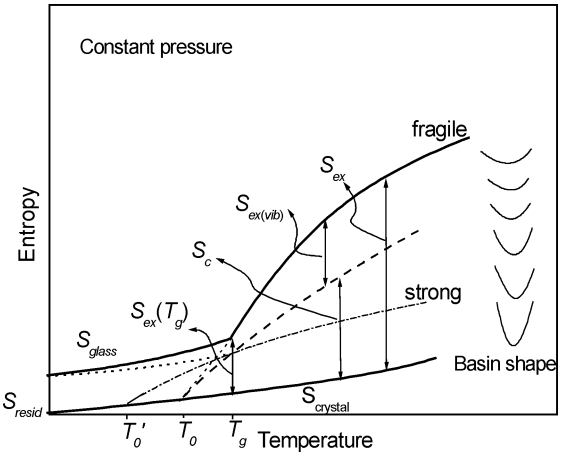


**Figure 2.** Changes in entropy of a system due to the change of the energy landscape "basin shape", that is, of the vibrational density of states during heating. The dash−dot line reflects the behavior of the liquid for which only the configurational excess entropy ($S_c$) makes the increase in enthalpy $H$. For the solid line above, the excited increasing configurational excess entropy as well as the vibrational part ($S_{ex(vib)}$) results in a much rapid increase in enthalpy, which makes the liquid behavior fragile. $T_0/T_g$ of a fragile liquid is larger than that of a strong liquid, $T_0'/T_g$.

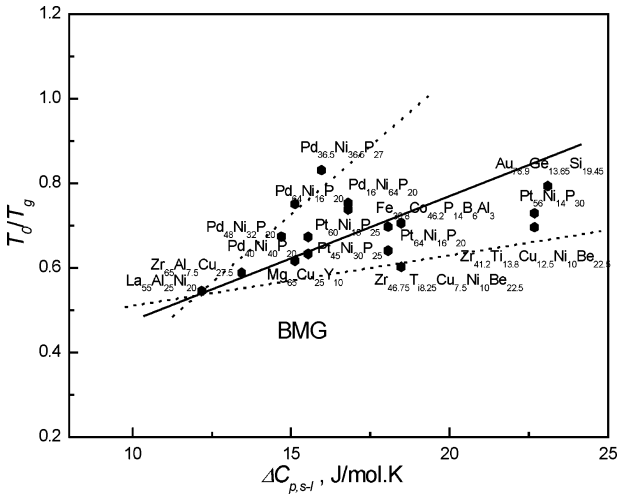


**Figure 3.** Value of $T_0/T_g$ vs the heat capacity changes caused by the glass transition, $\Delta C_{p,s-l}$, for different series of metallic glasses. Lines are guides to the eye. The solid line corresponds to an average trend. Dotted lines represent linear "bounds" displayed by the scattering of the points.

to the glass transition, $S_c(T_g)$. Although different explanations have been given to describe the meaning of $T_0$,[45,46] several authors of works about organic[47−50] and mineral substances[51−55] have found that the value of $T_0$ coincides with that of the Kauzmann temperature $T_K$ ($T_K$ is the ideal thermodynamic glass transition temperature and at $T_K$ the extrapolated configurational entropy of the supercooled liquid equals that of the crystal[56,57]). Notice that $T_g$ is the measured dynamic glass transition temperature. According to Figure 2, $T_K/T_g$ (or $T_0/T_g$) reflects the change in basin shape with basin energy. The larger $T_0/T_g$ is, the more the variable basin shape changes with temperature.

In Figure 3, we plot the ratio $T_0/T_g$ derived from the data in Table 1 against the corresponding values of $\Delta C_{p,s-l}$. The value of $T_0/T_g$ ranges from 0.55 to 0.93. In contrast, it is in the range of 0.44−1.16 for polymers and organic liquids.[58] Notice that here only bulk metallic glasses (BMG) are considered. Marginal metallic glasses (MMG) such as Al-based alloys are not taken into account. It is due to the lack of the supercooled liquid region

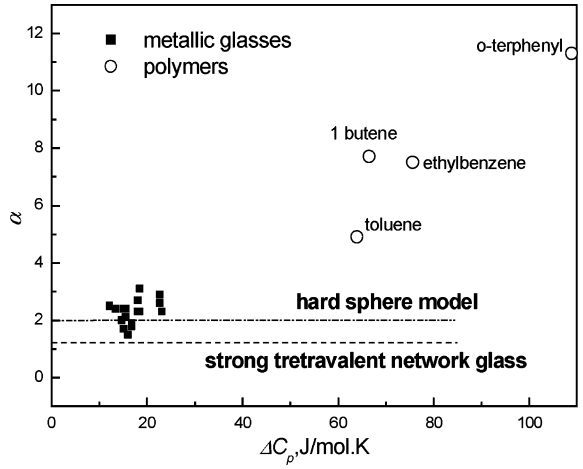


**Figure 4.** Values of α for different types of materials. Here the quantity α is a measure of the total number of inherent structures (individual minima of the potential energy hypersurface).[65] The metallic glasses correspond to those shown in Figure 3. The examples of polymers are taken from ref 66.

in the calorimetric scanning of the MMG,[37] as shown in Figure 1. For the MMG, $T_x$ is very similar to $T_g$, which results from the existence of the quenched-in prenuclei in the amorphous sample.[59,60] It causes that the region of the supercooled liquid cannot be observed and the structural relaxation near $T_g$ is incomplete before the crystallization process occurs. BMG, however, usually own a large supercooled region of even more than 150 K.[61] Thus, the real value of heat capacity difference between the supercooled liquid and the amorphous alloys for MMG should be larger than that depicted in Figure 1.

We notice that the plot of $T_0/T_g$ against $\Delta C_{p,s-l}$ does not indicate a perfect correlation; instead, it shows a scattering of the points around an average trend (represented by a solid line in Figure 3). According to Figure 2, the average trend shows that there exists a correlation between the increases of vibrational and configurational excess entropies toward $T_g$. It indicates that, as the structure changes above $T_g$, an increase in $S_{ex(vib)}$ due to the change in shape of the inherent structure basins that the system visits promotes a corresponding increase in configurational entropy, that is, the density of the basin minimum. However, the scattering of the points indicates that the quantitative correlation between the different parts of the excess entropy is material-dependent. It is also found that in Figure 3 the relationship between $T_0/T_g$ and $\Delta C_{p,s-l}$ tends to fall inside the two dotted lines. This phenomenon is believed to relate to the particular nature of atomic architecture in metallic materials, which may be demonstrated by a Gaussian model. A Gaussian distribution of the limiting densities of glasses has been successful in simulation studies of a tetravalent network model,[62] hard spheres,[63] and hard disk mixtures.[64] In the Gaussian curve that describes the distribution of energies, the height of the peak of the distribution, α, which corresponds to the high-temperature limit, usually determines the total number of glasses that the system can sample.[65] The values of α of the metallic glasses in Figure 3 can be calculated by using the following equation:[66]

$$\Delta C_{p,s-l}(\chi(T),T) = 2\alpha R(T_0/T)^2, \quad T > T_0 \qquad (2)$$

Here $T$ is displaced by $T_g$ in Table 1. Figure 4 gives the obtained values of α, as well as the values of other types of materials previously reported. As shown in Figure 4, the α of metallic glasses ranges from 1.6 to 3.0. In contrast, the α of more fragile polymers ranges widely from 4.9 to 11.3.[66] For a stronger

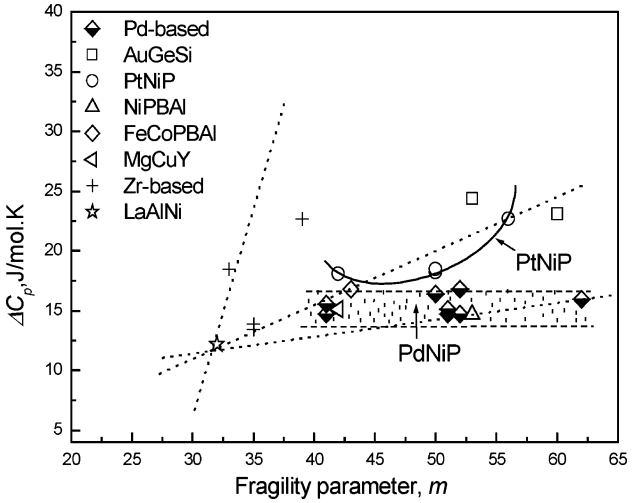


**Figure 5.** Heat capacity change at $T_g$, $\Delta C_{p,s-l}$, vs fragility parameter, $m$, for different systems of metallic glasses. The dotted line in the center represents linear regression through data. Other dotted lines represent "bounds" on the correlation. The solid curve and the dotted area between the dashed lines reflect, respectively, the behavior of the PtNiP system and the particularity of the PdNiP system.

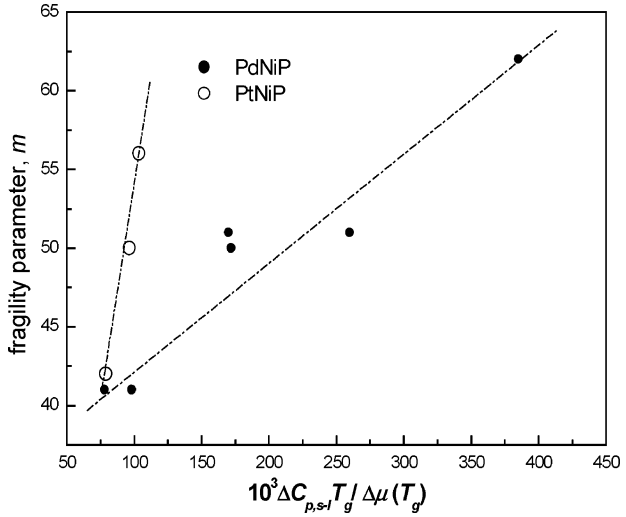


**Figure 6.** Fragility parameter, $m$, vs the calculated value of ($\Delta C_{p,s-l}T_g/\Delta\mu(T_g)$) for PdNiP and PtNiP metallic systems with different contents of compositions.

tetravalent network model, α is about 1.2, and for the intermediate fragile hard sphere fluid, α equals 2.[62,63] It is observed that the α of metallic glasses, which is just between the value of tetravalent network model and that of polymers, ranges around that of the hard sphere fluid. It makes us believe that the manner of atomic arrangements (similar to the hard sphere model) due to metallic bonds is the underlying reason the points in Figure 3 concentrate in the area between the two linear bounds. However, the idea that any metallic system (especially the type of MMG) cannot fall outside these bounds needs further investigation.

Although the hard sphere model for metallic glasses gives some information concerning the concentration of the points, at present we gain no insight into what is the origin of the scattering of the points yet. Since the total number of configurations (or density of energy basins) per $N$-particle system seems to be not very dependent on the nature of the interaction potential and roughly exponential with $N$, the scattering of the points uncovers the necessity to investigate the other features of PEL, which more depend on details of atomic interactions than the density of the energy minima that a system sample does (reflected by $\Delta C_{p,s-l}$).[67−69] In the following part, attempts are made to probe the dependence from other aspects.

**3.2. The Height of Energy Barriers Separating the Minima ($\Delta\mu$) and Mismatch Entropy ($S\sigma/k_B$) of Alloys.** Figure 5 shows the heat capacity change at $T_g$, $\Delta C_{p,s-l}$, vs fragility parameter, $m$, for different systems of metallic glasses. A generally positive relationship is found between $m$ and $\Delta C_{p,s-l}$, suggesting that large heat capacity difference between the glass and the supercooled liquid near $T_g$ corresponds to large liquid fragility. In the PEL, it means that the number of the energy basins of strong liquids seems much smaller than that of fragile ones. In this point, metallic glasses generally coincide with the idea proposed by Angell,[47] which is based on the previously investigated small molecular liquids and ionic glasses.[39,41,49]

However, in Figure 5, the slope of the positive correlation is not uniform, just similar to the phenomenon shown in Figure 3. In particular, as the dotted area in Figure 5 shows, the system of PdNiP metallic glasses with the similar $\Delta C_{p,s-l}$ (3.5−4.0 cal/mol·K) exhibits, however, large changes in the fragility strength ($m$: 41−62). The different families of behavior lie beyond what the error caused by different experimental conditions can explain. It suggests that, although $\Delta C_{p,s-l}$ is an dominant and positive factor, it is surely not the only one to determine liquid fragility strength, just as pointed out by Ruocco and Sciortino.[65] Notice that the change in $C_p$ reflects the density of minima at the level of the landscape at which the system gets trapped during cooling, and this level will depend on the height of energy barriers separating the minima as well as the total degeneracy. Thus, the height of energy barriers separating the minima, $\Delta\mu$, is another factor that should be taken into account. Fortunately, the values of $\Delta\mu$ for some metallic glasses can be calculated according to the values given in ref 19. Then we plot the value of ($\Delta C_{p,s-l}T_g/\Delta\mu(T_g)$) against that of $m$ for both PdNiP and PtNiP systems in Figure 6. Different from the dotted area (for PdNiP) and the solid curve (for PtNiP) in Figure 5, two dash−dotted beelines appear in Figure 6. This observation shows us that, for a system with different contents of compositions (for which $T_g$ is similar), the ratio of the number of potential energy minima to the height of the barrier between minima controls the liquid fragility, that is to say

$$m \propto k\Delta C_{p,s-l}(T_g)/\Delta\mu(T_g) \tag{3}$$

The finding agrees with Stillinger' idea of the possible importance of $\Delta\mu$ in determining fragility.[68] Besides, for different metallic systems, the slope, $k$, in eq 3 is different. Although the PtNiP system has a larger $k$ than the PdNiP system, its $T_g$ is smaller than the latter. It suggests that the glass transition temperature is independent of the fragility. The present results support our previous idea based on the fragility of the AlNiCe alloys that to specify the dynamics of a system in the glass transition region one needs both the glass transition temperature and the liquid fragility strength.[17]

Then in order to explore how the change of chemical structural determinants influences the $\Delta\mu$ in the PEL, we focus on the Pd-based glasses. Their similar values of $\Delta C_{p,s-l}$ allow us to ignore the density of energy minima in the landscape and focus on the feature of $\Delta\mu$ by investigating $m$. Notice that all of the basic features of the PEL have their own chemical basis. By investigation on covalent, molecular, and polymeric liquids, Rao[70] has demonstrated that electronegativities and bond distances between elements are two important parameters that can be used to determine liquid fragility. It is a pity that how

**TABLE 2: Mixing Enthalpy ($\Delta H^{chem}$, KJ/Mol), Mismatch Entropy ($S_\sigma/k_B$) and the Fragility Value ($m$) of Amorphous Alloys of the PdNiP System[a]**

| metallic glasses | $m$ | $\Delta H^{chem}$ | $S_\sigma/k_B$ | $\Delta\mu$ |
|---|---|---|---|---|
| $Pd_{36.5}Ni_{36.5}P_{27}$ | 62 | −28 | 0.17 | 6.270 |
| $Pd_{37.5}Ni_{37.5}P_{25}$ | 51 | −27 | 0.16 | 8.260 |
| $Pd_{64}Ni_{16}P_{20}$ | 51 | −23 | 0.15 | 15.192 |
| $Pd_{16}Ni_{64}P_{20}$ | 50 | −22 | 0.15 | 16.580 |
| $Pd_{48}Ni_{32}P_{20}$ | 41 | −21 | 0.14 | 20.720 |
| $Pd_{40}Ni_{40}P_{20}$ | 41 | −21 | 0.14 | 27.435 |

[a] The values of the minimum activation energy of a rearrangeable region ($\Delta\mu$, kcal/mol) are calculated according to ref 19.

to determine the two parameters for metallic glasses is not given. However, inspired by his work, we selected the mismatch entropy normalized by Bolzmann constant ($S_\sigma/k_B$) and the chemical mixing enthalpy ($\Delta H^{chem}$) as the discussed objects. The two quantities reflect, respectively, the significant difference in atomic size ratios and the negative heats of mixing among the constituent elements related to the bond strength. More important is that they are both functions of content of the compositions in a multicomponent system. It makes the investigation inside one system (such as PdNiP) into reality.

On the basis of the extended regular solution model, chemical mixing enthalpy and mismatch entropy are calculated according to eqs 4 and 5:[71]

$$\Delta H^{chem} = \sum_{\substack{i=1 \\ i\neq j}}^{3} \Omega_{ij} c_i c_j \tag{4}$$

$$S_\sigma/k_B = \frac{3}{2}(\varsigma^2 - 1)y_1 + \frac{3}{2}(\varsigma - 1)^2 y_2 - \left[\frac{1}{2}(\varsigma - 1)(\varsigma - 3) + \ln \varsigma\right](1 - y_3) \tag{5}$$

Here $\Omega_{ij}$ is the regular solution interaction parameter between the $i$th and $j$th elements; $c_i$ is the composition of the $i$ element; $k_B$ is the Boltzmann constant; $\zeta$ is a constant which reflects a dense random packing. For the detailed description of $\Omega_{ij}$ and the dimensionless parameters ($y_1$, $y_2$, $y_3$), please see ref 71. The atomic diameters of Pd, Ni, and P elements are quoted from ref 72.

Table 2 lists the calculated values of $\Delta H^{chem}$ and $S_\sigma/k_B$ for the investigated PdNiP system with different contents of compositions. In Table 2, we can see, with the $\Delta\mu$ increasing, the PdNiP alloys present a tendency for $S_\sigma/k_B$ to decrease with increasing $\Delta H^{chem}$. The tendency of the change of $\Delta\mu$ is completely opposite to that of $S_\sigma/k_B$. Considering the close relationship between $S_\sigma/k_B$ and $\Delta H^{chem}$ just as discussed in ref 71, here we will pay attention to one quantity, $S_\sigma/k_B$. Table 2 displays for us that mismatch entropy is closely related to the height of energy barriers between minima. Underlying the observation is that the low height of energy barriers results from large differences in atomic size between constituent atoms. Since significant differences in atomic size can result in high coordination numbers, it can be deduced that when the atoms have high coordination numbers, lower energy barriers can result and consequently the rearrangement of the structural regions (or the clusters) will be easy. Our previous work[17] has shown that for the AlNiCe system large liquid fragility is due to unstable clusters in their liquids. To further verify the correlation between the cluster stability and the mismatch entropy due to the nature of the atoms, we give the values of $\Delta H^{chem}$ and $S_\sigma/k_B$ for the AlNiCe alloys, as shown in Table 3. It can be seen

**TABLE 3: Absolute Value of Mixing Enthalpy ($\Delta H^{chem}$, kJ/mol) and Mismatch Entropy of Amorphous Alloys in the AlNiCe System Calculated According to Ref 71, Where the Cluster Stability of the Glasses Is Taken from Ref 17**

| metallic glasses | $\lvert\Delta H^{chem}\rvert$ | $S_\sigma/k_B$ | cluster stability |
|---|---|---|---|
| $Al_{87}Ni_{10}Ce_3$ | 12 | 0.11 | ↓ |
| $Al_{85}Ni_{10}Ce_5$ | 15 | 0.13 | |
| $Al_{84}Ni_{10}Ce_6$ | 16 | 0.14 | gradually decrease |
| $Al_{82}Ni_{10}Ce_8$ | 18 | 0.17 | |

that the increasing $S_\sigma/k_B$ decreases the cluster stability, and then the AlNiCe alloy system exhibits the same tendency as the PdNiP family. Thus, for metallic glasses the height of energy barrier among neighboring minima is determined by the large difference in atomic size of the component atoms displayed by the chemical mismatch entropy. The importance of the entropy dependence of $\Delta\mu$ may also be detected by the theoretical equation proposed by Robin[66]

$$\Delta C_{p,s-l}(T_g) = (f - 1)\Delta S_{s-l}(T_g) \tag{6}$$

in which $f$, another differently defined dynamic fragility parameter, has a meaning similar to $m$; the subscript s−l means the transition from amorphous solids to supercooled liquids. Comparison between eqs 3 and 6 shows that the entropic factor is indeed a dominant factor in influencing the barrier height between energy minima.

There is another question worthy to be pointed out. Generally $S_\sigma/k_B$ and $\Delta H^{chem}$ are good criterions to evaluate the glass-forming ability (GFA) of metallic alloys. Large $S_\sigma/k_B$ displays high GFA. In both Tables 2 and 3 large $S_\sigma/k_B$ (or absolute value of $\Delta H^{chem}$) corresponds to large $m$. Then one question that people have been interested in presents itself: is there a general relationship between the liquid fragility and the GFA? Since liquid fragility manifests the easiness of the structural changes toward $T_g$, it is often believed that the liquid with large fragility strength should have a bad GFA. However, here the findings show that the idea is deficient. For PdNiP alloys, the relationship is completely opposite to what people expected. The same circumstance has also been found in other two Pd-based metallic glasses, $Pd_{40}Ni_{40}P_{20}$ and $Pd_{43}Cu_{27}Ni_{10}P_{20}$,[73] as well as in Al-based alloys.[74] Consequently, the idea that the manner (growth-controlled or nucleation-controlled vitrification conditions) is the main factor to determine the relationship between the liquid fragility and the GFA of metallic alloys is further verified.

## 4. Conclusions

In summary, an average trend between $T_0/T_g$ and heat capacity changes due to the glass transition indicates that the more rapidly the landscape is ascended, the more rapidly the configurational entropy is excited. It in some degree verifies the idea proposed to explain the satisfactions of both the total excess entropy and the configuration part in the Adam−Gibbs equation. Although the dynamic fragility strength is closely related to the heat capacity changes at $T_g$, analysis of PdNiP and PtNiP systems shows that the liquid fragility can be better expressed by the ratio of the number of the energy basins to the averge height of energy barriers between minima near the glass transition. Analysis of the PdNiP alloys with different contents of compositions, as well as the AlNiCe system, makes us believe that the mismatch entropy is a dominant factor in the height of energy barriers between minima. It implies that metallic glass formers have a PEL that is sensitive to entropic effects and that the entropic glass transition can be viewed as an excellent descriptor of material behavior. In this point, metallic glasses

seem different from the polymeric glass formers for which volumetric factors are more considered.

**Acknowledgment.** This work was supported by National Natural Science Foundation of China (Grant No. 50231040; Grant No. 50301008) and Natural Science Foundation of Shandong province (Grant No. Z2004F02).

## References and Notes

(1) Michael J. T. *Chem. Geol.* **2001**, *174*, 321.
(2) Alba-simionesco, C. *C. R. Acad. Sci. Paris*, **2001**, *2* (IV), 203.
(3) Wilde, G. *J. Non-Cryst. Solids.* **2002**, 307−310, 853.
(4) Kauzmann, W. *Chem. Rev.* **1948**, *43* (2), 219.
(5) Adam, G.; Gibbs, J. H. *J. Chem. Phys.* **1965**, *43*, 139.
(6) Stillinger, F. H.; Debenedetti, P. G. *J. Chem. Phys.* **2002**, *116*, 3353.
(7) Sastry, S.; Debenedetti, P. G.; Stillinger, F. H. *Nature (London)* **1998**, *393*, 554.
(8) Heuer, A. *Phys. Rev. Lett.* **1997**, *78*, 4051.
(9) Angelani, L.; Parisi, G.; Ruocco, G.; Viliani, G. *Phys. Rev. Lett.* **1998**, *81*, 4648. Angelani, L.; Leonardo, R. D.; Ruocco, G.; Scala, A.; Sciortino, F. *Phys. Rev. Lett.* **2000**, *85*, 5365.
(10) Coluzzi, B.; Parisi, G.; Verocchio, P. *Phys. Rev. Lett.* **2000**, *84*, 306.
(11) Sciortino, F.; Kob, W.; Tartaglia, P. *Phys. Rev. Lett.* **1999**, *83*, 3214.
(12) Schroder, T. B.; Sastry, S.; Dyre, J.; Glotzer, S. C. *J. Chem. Phys.* **2000**, *112*, 9834.
(13) Michael, S. *Phys. Rev. B* **1998**, *57*, 11319.
(14) Hu, L. N.; Bian, X. F. *Chin. Sci. Bull.* **2004**, *49*, 1.
(15) Oren, M. B.; Martin, K. *J. Chem. Phys.* **1997**, *106*, 1495.
(16) Martinez, L. M.; Angell, C. A. *Nature (London)* **2001**, *410*, 663.
(17) Hu, L. N.; Bian, X. F.; Wang, W. M.; Zhang, J. Y.; Jia, Y. B. *Acta Mater.* **2004**, *52*, 4773.
(18) Kieran, J. C.; George, Z. *Thermochim. Acta* **2001**, *380*, 79.
(19) Chen, H. S. *J. Non-Cryst. Solids* **1978**, *29*, 223.
(20) Perera, D. N. *J. Phys.: Condens. Matter.* **1999**, *11*, 3807.
(21) Kawamura, K.; Inoue, A. *Appl. Phys. Lett.* **2000**, *77*, 1114.
(22) Chen, H. S. *J. Non-Cryst. Solids.* **1978**, *27*, 257.
(23) Chen, H. S.; Goldstein, M. *J. Appl. Phys.* **1972**, *43*, 1642.
(24) Chen, H. S. *J. Non-Cryst. Solids.* **1976**, *22*, 135.
(25) Hu, X.; Tan, T. B.; et al. *J. Noncryst. Solids.* **1999**, *260*, 228.
(26) Busch, R.; Liu, W.; Johnson, W. L. *J. Appl. Phys.* **1998**, *83*, 4134.
(27) Busch, R.; Mashur, A.; Johnson, W. L. *Mater. Sci. Eng. A* **2001**, *304−306*, 97.
(28) Waniuk, T. A.; Busch, R.; Masuhr, A.; Johnson, W. L. *Acta Mater.* **1998**, *46*, 5229.
(29) Kambousky, M.; Moske, K. S. *Z. Physica B* **1996**, *99*, 387.
(30) Reinker, B.; Dopfer, M.; Moske, M. *Eur. Phys. J. B: Condens. Matter.* **1999**, *7*, 359.
(31) Busch, R *Ann. Chim.—Sci. Mater.* **2002**, *27*, 3.
(32) Bakke, E.; Busch, R.; Johnson, W. L. *Appl. Phys. Lett.* **1995**, *67*, 3260.
(33) Okumura, H.; Inoue, A.; Masumoto, T. *Mater. Trans., JIM* **1991**, *32*, 593.
(34) Chen, H. S.; Turnbull, D. *J. Chem. Phys.* **1968**, *48*, 2560.
(35) Angell, C. A. *J. Non-Cryst. Solids.* **1991**, *131−133*, 13.
(36) Kivelson, D.; Tarjus, G.; Zhao, X.; Kivelson, S. A. *Phys. Rev. E* **1996**, *53*, 751.
(37) Wilde , G.; Boucharat , N.; Hebert , R. J.; Rösner , H.; Tong , W. S.; Perepezko , J. H. *Adv. Eng. Mater.* **2003**, *5*, 125.
(38) Zhou, S. H.; Schmid, J.; Sommer, F. *Thermochim. Acta* **1999**, *339*, 1.
(39) Böhmer, R.; Ngai, K. L.; Angell, C. A.; Plazek, D. J. *J. Chem. Phys.* **1993**, *99*, 4201.
(40) Komatsu, T. *J. Non-Cryst. Solids* **1995**, *185*, 199.
(41) Angell, C. A.; Richards, B. E.; Velikov, V. *J. Phys: Condens. Matter* **1999**, *11* (10A), 75.
(42) Green, J. L.; Ito, K.; Xu, K.; Angell, C. A. *J. Phys Chem. B* **1999**, *103*, 3991.
(43) Sokolov, A. P.; Rossler, E.; Kisliuk, A.; Quitmann, D. *Phys. Rev. Lett.* **1993**, *71*, 2062.
(44) Roland, C. M.; Santangelo, P. G.; Ngai, K. L. *J. Chem. Phys.* **1999**, *111*, 5593.
(45) Novikov, V. N.; Rössler, E.; Malinovsky, V. K.; Surovtsev, N. V. *Europhys. Lett.* **1996**, *35*, 289.
(46) Jeppe, C. D. *J. Non-Cryst. Solids.* **1998**, *235−237*, 142.
(47) Angell, C. A. *J. Non-Cryst. Solids.* **1988**, *102* (1−3), 205.
(48) Angell, C. A. *Polymer* **1997**, *38*, 6261.
(49) Angell, C. A. *Science* **1995**, *267*, 1924.
(50) Angell, C. A.; Rao, K. J. *J. Chem. Phys.* **1972**, *57*, 470.
(51) Odagaki, T. *Phys. Rev. Lett.* **1995**, *75*, 3701.
(52) Klose, G.; Fetch, H. J. *Mater. Sci. Eng., A* **1998**, *179&180*, 77.
(53) Fecht, H. J.; Perepezko, J. H.; Lee, M. C.; Johnson, W. L. *J. Appl. Phys.* **1990**, *68*, 4494.
(54) Angell, C. A. *J. Res. Natl. Inst. Stand. Technol.* **1997**, *102*, 171.
(55) Angell, C. A. *Physica D.* **1997**, *107*, 122.
(56) Angell, C. A.; Tucker, J. C. *J. Phys. Chem.* **1974**, *78*, 278.
(57) Gibbs, J. H.; Di Marzio, E. A. *J. Chem. Phys.* **1958**, *28*, 373.
(58) Rault, J. *J. Non-Cryst. Solids.* **2000**, *271*, 177.
(59) Perepezko, J. H.; Hebert, R. J.; Wu, R. I.; Wilde, G. *J. Non-Cryst. Solids.* **2003**, *317*, 52.
(60) Inoue, A. *Prog. Mater. Sci.* **1998**, *43*, 365.
(61) Lu, Z. P.; Li, Y.; Ng, S. C.; Feng, Y. P.; Lu, K. *J. Non-Cryst. Solids.* **1998**, *250−252*, 689.
(62) Speedy, R. *J. Mol. Phys.* **1996**, *88*, 1293.
(63) Speedy, R. *J. Mol. Phys.* **1998**, *95*, 165.
(64) Speedy, R. J. *J. Chem. Phys.* **1999**, *110*, 4559.
(65) Ruocco, G.; Sciortino, F. *J. Chem. Phys.* **2004**, *120*, 10666.
(66) Robin, J. S. *J. Phys. Chem. B* **1999**, *103*, 4060.
(67) Stillinger, F. H. *Phys. Rev. E* **1999**, 59, 48.
(68) Stillinger, F. H. *Science* **1995**, *267*, 1935.
(69) Ball, K. D.; Berry, R. S.; Kuntz, R. E.; Li, F. Y.; Proykova, A.; Wales, D. J. *Science* **1996**, *271*, 963.
(70) Rao, K. J.; Kumar, S.; Bhat, M. H. *J. Phys. Chem. B* **2001**, *105*, 9023.
(71) Takeuchi, A.; Inoue, A. *Mater. Trans., JIM* **2000**, *41*, 1372.
(72) Smithells, C. J.; Brandes, E. A. *Metals Reference Book*, 5th ed., Butterworths: Boston, MA, 1976; p 100.
(73) Wilde, G. *J. Non-Cryst. Solids.* **2002**, 312−314, 537.
(74) Si, P. C.; Bian, X. F.; Zhang, J. Y.; Li, H.; Sun, M. H.; Zhao, Y. *J. Phys.: Condens. Matter* **2003**, *15*, 5409.